ASTEROID PROXIMITY GNC ASSESSMENT THROUGH HIGH-FIDELITY ASTEROID DEFLECTION EVALUATION SOFTWARE (HADES)

Massimo Vetrisano and Juan L. Cano
{massimo.vetrisano, juan-luis.cano}@deimos-space.com

The 6th International Conference on Astrodynamics Tools and Techniques (**ICATT**)

Why HADES?

Motivations

- Increasing number of missions to minor bodies (science, deflection)
- Relatively unknown environment (lack of knowledge prior arrival)
- Detailed preliminary analysis (operational orbit)
- System performance (e.g. thruster accuracy, sensors)

High-fidelity Asteroid Deflection Evaluation Software* capabilities

- Analysis of spacecraft motions at irregular objects
- Performance of different types of guidance schemes
- Relative navigation methods
- Performance of slow-push asteroid threat mitigation methods as Gravity Tractor (GT), Ion-beam Shepherd (IBS) and Laser Ablation (LA)

***Hades** (/ˈheɪdiːz/; Ancient Greek: ᾍδης or Ἅιδης, *Háidēs*) ancient Greek chthonic god of the underworld

Software Architecture

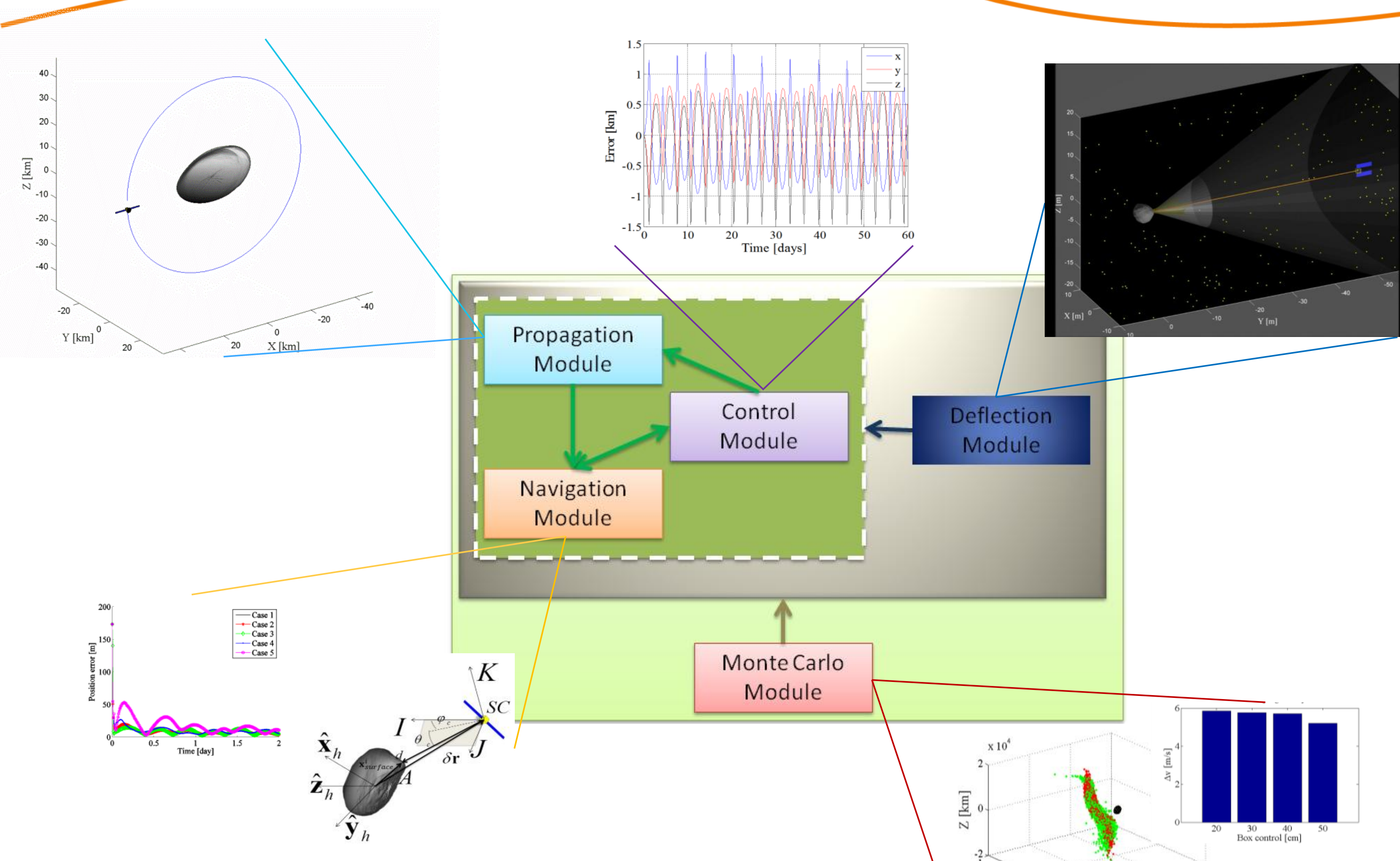

HADES is a full Matlab software relying on a number of C routines

Propagation Module: Spacecraft Dynamics

elecnor deimos

- Hill' s frame

$$\ddot{\mathbf{r}} + 2\dot{\boldsymbol{\theta}}\mathrm{x}\dot{\mathbf{r}} + \dot{\boldsymbol{\theta}}\mathrm{x}(\dot{\boldsymbol{\theta}}\mathrm{x}\mathbf{r}) = -\frac{\mu_a}{r^3}\mathbf{r} + \mu_{Sun}\left(\frac{\mathbf{r_a}}{\mathbf{r_a^3}} - \frac{\mathbf{r_{sc}}}{\mathbf{r_{sc}^3}}\right) + \frac{\partial U}{\partial(\delta\mathbf{r})} + \boldsymbol{SRP}(\mathbf{r_{sc}}) + \mathbf{u}$$

- Asteroid's frame

$$\ddot{\boldsymbol{r}} = -\frac{\mu_a}{\delta r^3}\boldsymbol{r} + \mu_{Sun}\left(\frac{\boldsymbol{r_a}}{r_a^3} - \frac{\boldsymbol{r_{sc}}}{r_{sc}^3}\right) + \frac{\partial U}{\partial(\delta\boldsymbol{r})} + SRP(\boldsymbol{r_{sc}}) + \boldsymbol{u}$$

- Body fixed frame

$$\ddot{\mathbf{r}} + 2\boldsymbol{\omega}\mathrm{x}\dot{\mathbf{r}} + \boldsymbol{\omega}\mathrm{x}(\boldsymbol{\omega}\mathrm{x}\mathbf{r}) = -\frac{\mu_a}{r^3}\mathbf{r} + \mu_{Sun}\left(\frac{\mathbf{r_a}}{\mathbf{r_a^3}} - \frac{\mathbf{r_{sc}}}{\mathbf{r_{sc}^3}}\right) + \frac{\partial U}{\partial(\delta\mathbf{r})} + \boldsymbol{SRP}(\mathbf{r_{sc}}) + \mathbf{u}$$

- Perturbation
  - SRP $\quad SRP(\boldsymbol{r_{sc}}) = C_r S_{srp}\left(\frac{r_{1AU}}{r_{sc}}\right)^2 \frac{\boldsymbol{r_{sc}}}{r_{sc}}\frac{A}{m_{sc}}$
  - Non uniform gravity field

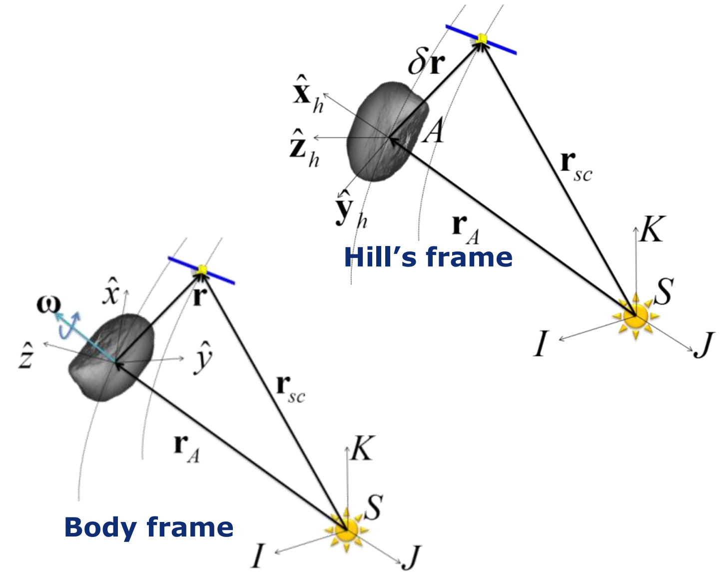

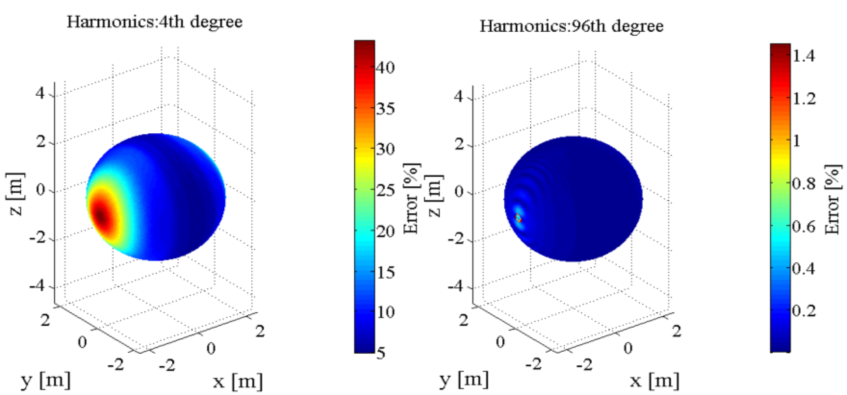

Relative error between harmonics and shape model

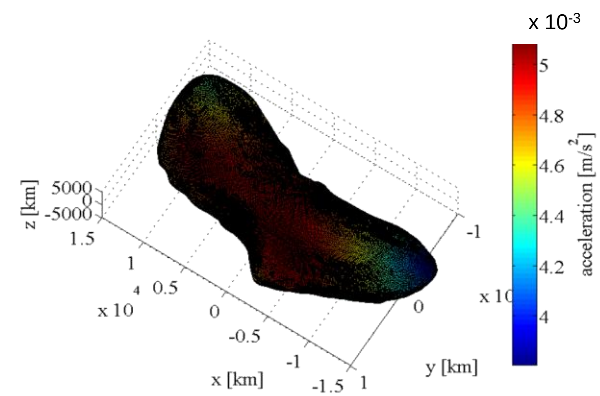

Shape model gravity acceleration on (433) Eros

Control Module

- A continuous Lyapunov controller

- Discrete controllers based on the concept of control box

- Discrete control based on reflection method
  - invert the direction of the velocity when the spacecraft gets closer,
  - apply a manoeuvre along the radial direction such as to obtain the velocity reflected with respect to the tangential direction

- Discrete control based on dead band control

- Discrete LQR with integrative contribution

- Discrete control designed using stability criteria (Y. Liu et al, 2003)

Manoeuvre error in magnitude and direction $\boldsymbol{u} = \boldsymbol{R}(\theta, \varphi)\boldsymbol{u}_{nom}(1 + r_{ex})$

❑ Problem definition

- Dynamics problem $x_{k+1} = f(x_k, u_k, w_k)$
- Measurements $y_k = h(x_k, v_k)$
- Estimate state variables $\tilde{\mathbf{x}}_k$

❑ Performance model $\mathbf{z} = [\mathrm{r}\ \mathrm{v}] + \mathbf{x}_{\mathrm{meas}}$

❑ **H-infinity** bounds the maximum expected error with unknown statistics

$$\mathbf{z}_k = \mathbf{L}_k x_k$$

$$J_h = -\frac{1}{\rho}\|\mathbf{x}_0 - \tilde{\mathbf{x}}_0\|^2_{P_0^{-1}} + \sum_{k=0}^{N-1}\left(\|\mathbf{z}_k - \tilde{\mathbf{z}}_k\|^2_{S_k} - \frac{1}{\rho}\left(\|\mathbf{w}_k\|^2_{Q_k^{-1}} + \|\mathbf{v}_k\|^2_{R_k^{-1}}\right)\right) < 1 \qquad J_h^* = \min_{\tilde{\mathbf{x}}_k}\ \max_{\mathbf{w}_k, \mathbf{v}_k, \mathbf{x}_0} J_h$$

- weighted samples to propagate mean and covariance matrix through sigma-points

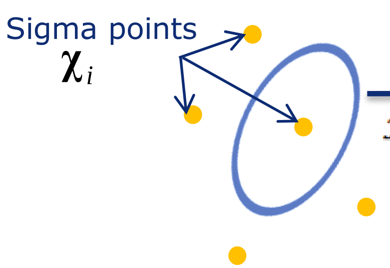

$$x^i_{k|k-1} = f(x^i_{k-1}, u_k)$$

$$\tilde{\mathbf{x}}_k^- = \sum_{i=0}^{2n} W_i^{(m)} x^i_{k|k-1}$$

$$\mathbf{P}_k^- = \sum_{i=0}^{2n} W_i^{(c)} \left(x^i_{k|k-1} - \tilde{\mathbf{x}}_k^-\right)\left(x^i_{k|k-1} - \tilde{\mathbf{x}}_k^-\right)^T$$

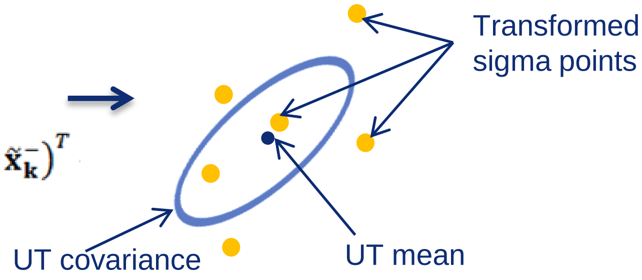

- update $\tilde{\mathbf{x}}_k = \tilde{\mathbf{x}}_k^- + \mathbf{K}(\mathbf{y}_k - \tilde{\mathbf{y}}_k^-)$ $\quad (P_k)^{-1} = (P_k^-) + (P_k^-)^{-1} P_{xy,k} R_k^{1-}\left[(P_k^-)^{-1}\mathbf{P}_{xy,k}\right]^T - \theta_k I_d$
- performance bound $\theta_k^{-1} = \xi\max\left(\mathrm{eig}\left(\left((P_k^-)^{-1}(P_k^-)^{-1} P_{xy,k} R_k^{1-}\left[(P_k^-)^{-1}\mathbf{P}_{xy,k}\right]^T\right)^{-1}\right)\right)$, Filter Gain $\mathbf{K} = \mathbf{P}_{xy,k}\mathbf{P}_{y,k}^{-1}$

Navigation Module: Measurements Model

- Camera and LIDAR models
  - Simple based on ellipsoidal shape
    - Centroid identification (x_c,y_c)
    - Local azimuth and elevation
    - LIDAR pointing towards the centroid

$$\phi = \tan^{-1}\frac{x_c^2}{f}$$

$$\psi = \tan^{-1}\frac{y_c^2}{\sqrt{(x_c^c)^2 + f^2}}$$

$$d = \left\| \delta r_{SC} - x_{surface}^c \right\|$$

  - Detailed based on actual shape models
    - Centre of brightness identified on the camera screen
    - LIDAR illuminates a spot close to the centre of brightness

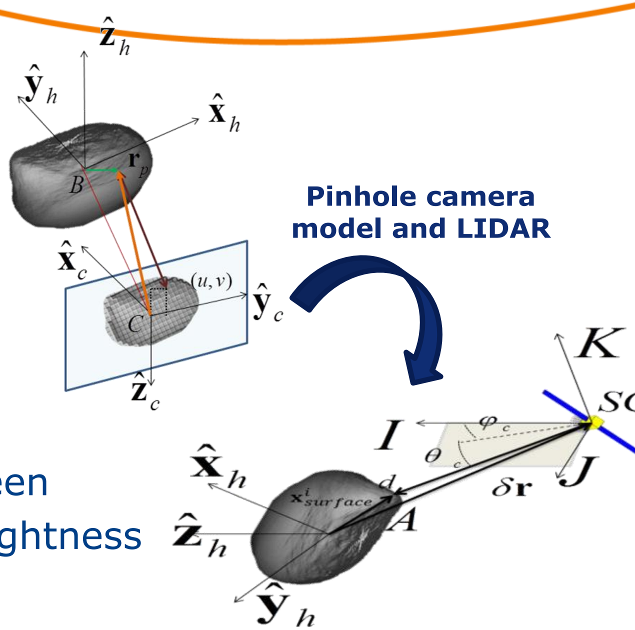

Pinhole camera model and LIDAR

- Modelisation of illumination and visibility

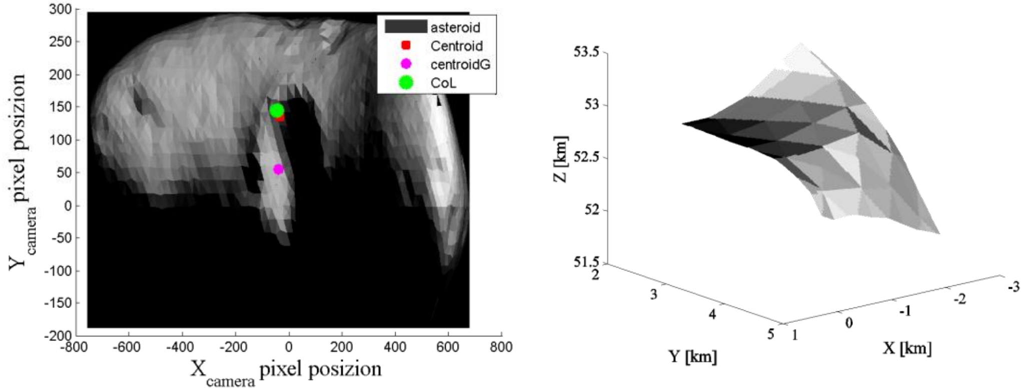

Example of image as seen on the screen of the camera and footprint of the LIDAR

Body Fixed with Asteroid Didymos

- Fixed hovering at 200m along a-axis
  - asteroid size $[c_1\ c_2\ c_3] = [1.05\ 0.65\ 0.45]\text{km}$
  - 4th order gravity field

- 100 m position error
- 1 cm/s velocity error
- 2% (3σ) error in magnitude
- 1.5 deg (3σ) error in direction

- 20 m along track (1σ)
- 10 m cross track (1σ)
- 2 mm/s along track (1σ)
- 1 mm/s cross track (1σ)

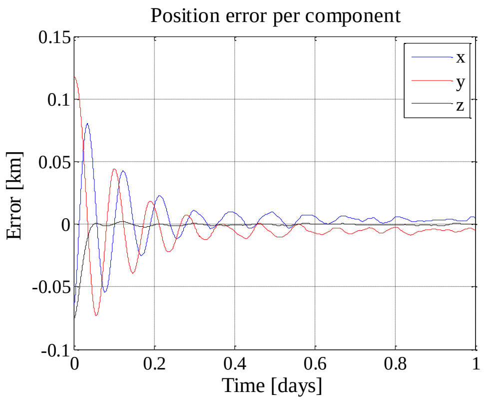

Continuous Thrust

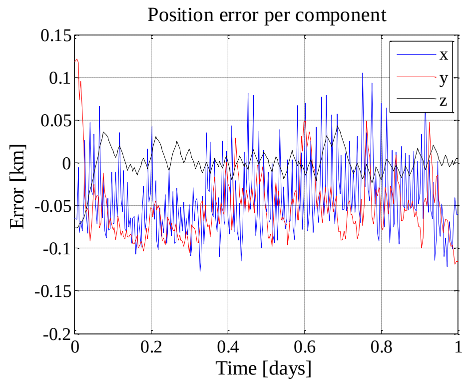

Control box with 300 s sampling time

Δv budget for 1 day

Method	Actuation interval	Δv [m/s]
Continuous thrust	5	56.2
Control box (100m)	300	62.5
Dead-band control (100m)	300	64.3
	600	61.7
	900	54.4
Discrete LQR	300	55.8
	600	54.9
	900	53.4
	1200	51.2

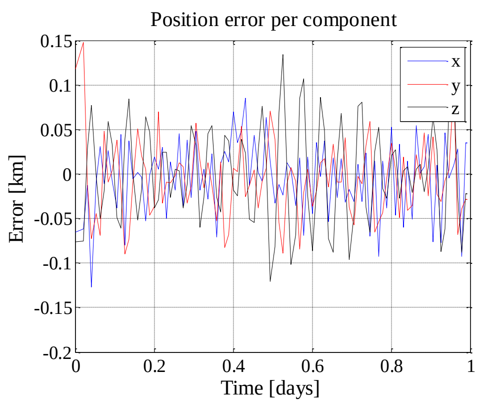

Dead-band with 900 s sampling time

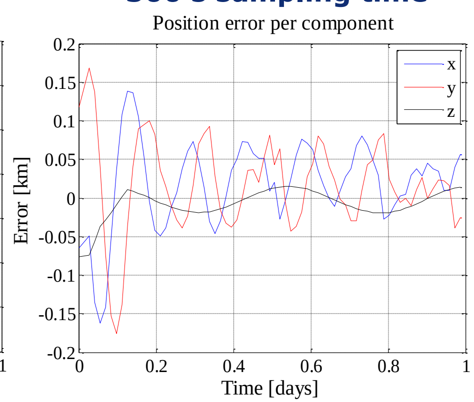

1200 s Discrete LQR

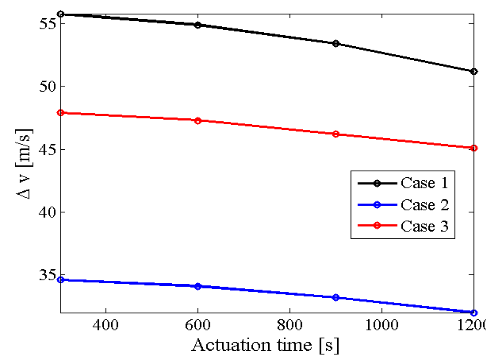

LQR for hovering 1) 200 above *a*, 2) 200 m above *b*, 3) 3D position 1300 m

Hill's Hovering: Controlling the Illumination Angle

❑ Objective: to maintain 5 degrees illumination angle

- Reference trajectory
  $x_{ref} = [-3.373km, 0km, 0km, 0km/s, 0km/s, 0km/s]$
- Initial trajectory
  $x_0 = [-3.423km, 0.05km, 0.05km, 0.000031km/s, -0.000051km/s, 0.000020km/s]$
- 4th order gravity field

- 2% (3σ) error in magnitude
- 1.5 deg (3σ) error in direction

- 20 m along track (1σ)
- 10 m cross track (1σ)
- 2 mm/s along track (1σ)
- 1 mm/s cross track (1σ)

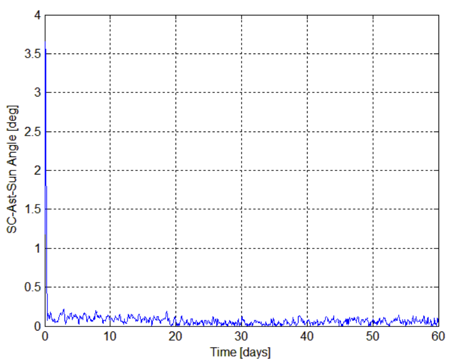

Continuous Thrust

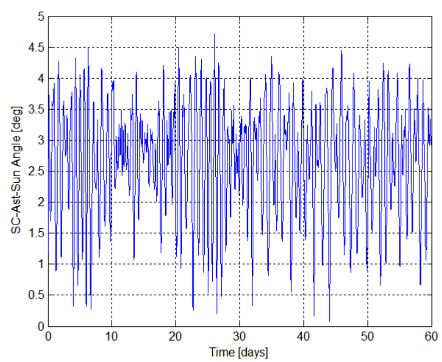

Control box

Δv budget for 60 days

Method	Actuation interval (min-max-mean) [min]	Δv [m/s]
Continuous thrust	8	16.9
Control box	421/533/485	24.2
Reflection method	325/1792/890	11.2
Dead-band control	8/440/140	25.9
Discrete LQR	360 (fixed)	24.1
Discrete LQR	240 (fixed)	24.0
Discrete LQR	180 (fixed)	23.1
Stable PD	360 (fixed)	18.2
Stable PD	240 (fixed)	18.2
Stable PD	180 (fixed)	18.2

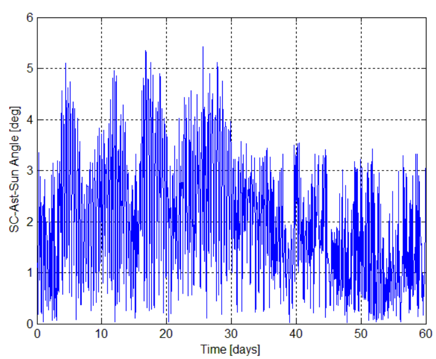

Dead-band

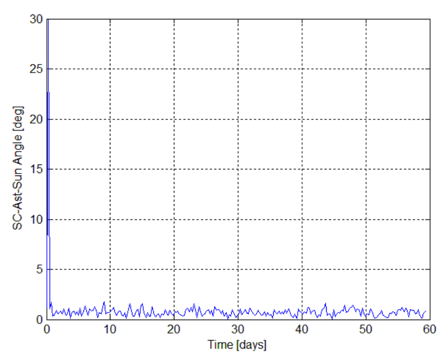

6 hrs discrete LQR

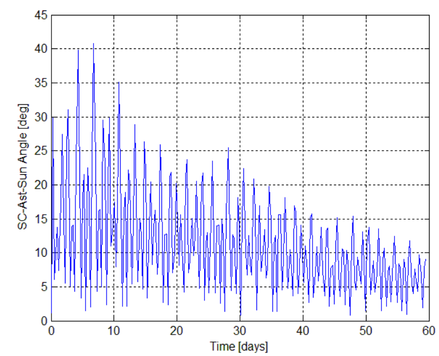

6 hrs stable PD

Hill's hovering: Navigation Errors

- Fixed hovering
  - Initial and reference trajectory
    $x_0 = 5 \cdot [-1km, 1km, \sqrt{2}km, 0km/s, 0km/s, 0km/s]$
  - 100 m initial position estimate error
  - 1 cm/s initial velocity error

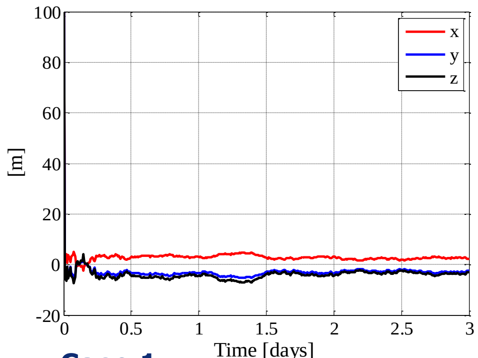

Case 1:
- True world ->ellipsoid shape
- Filter 4th order gravity field
- Measurements model simple

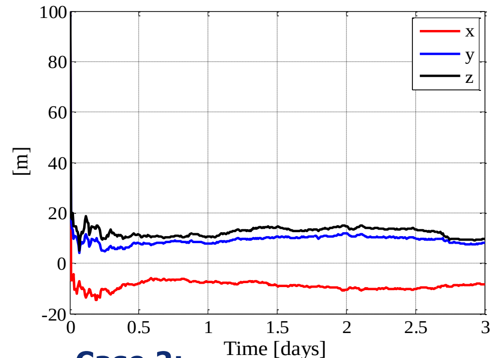

Case 2:
- True world ->ellipsoid shape
- Filter 4th order gravity field
- Measurements model detailed

Measurements assembly characteristics

Lidar mounting error (1σ)	0.001 deg
Lidar range error (1σ)	10 m
Lidar range bias (1σ)	1 m
Number of pixels per side	2048
Camera FoV	20 deg
Camera side	10 cm
Attitude error (1σ)	0.0057 deg
Attitude bias (1σ)	0.0006 deg

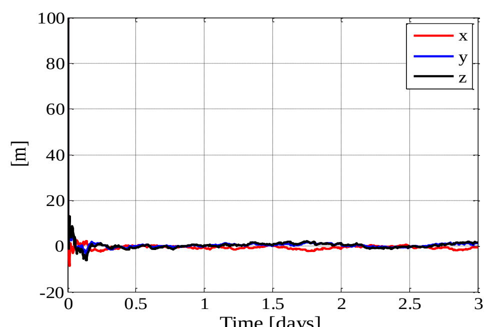

Case 3:
- True world ->1708 facets*
- Filter ->1708 facets*
- Measurements model detailed

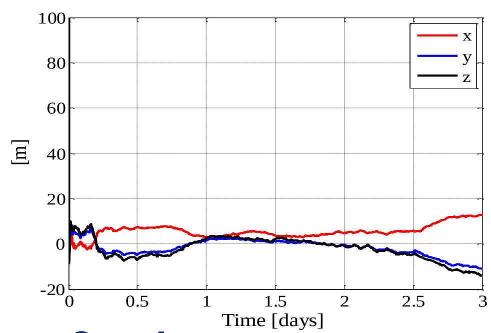

Case 4:
- True world -> 7790 facets*
- Filter ->1708 facets*, 1% error on R_{mean}
- Measurements model detailed

Δv budget for 3 day

	Δv [cm/s]
Case 1	9.18
Case 2	9.14
Case 3	9.25
Case 4	9.18

- 10% difference between different models

*shape from asteroid (433) Eros

Station Keeping at 10 km Station for AIM

- Initial trajectory

$$x_0 = 5 \cdot [-1km, 1km, \sqrt{2}km, 0km/s, 0km/s, 0km/s]$$

- Control box 1.5 km side
  - 2% (3σ) error in magnitude
  - 1.5 deg (3σ) error in direction
- Performance model
  - 20 m along track (1σ)
  - 10 m cross (1σ)
  - 2 mm/s along track (1σ)
  - 1 mm/s along track (1σ)

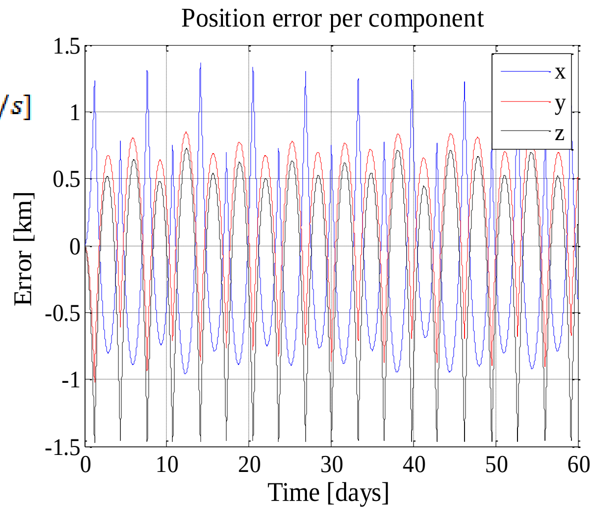

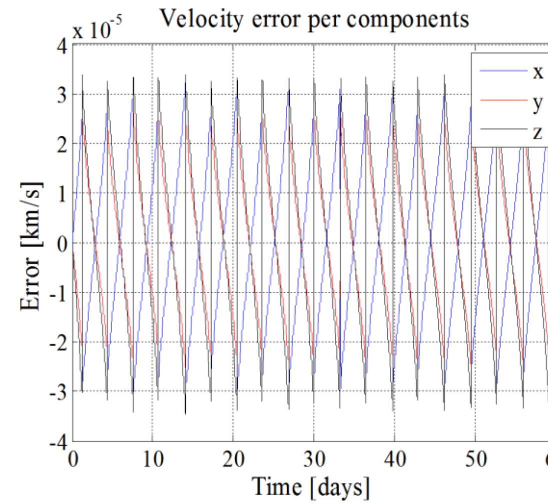

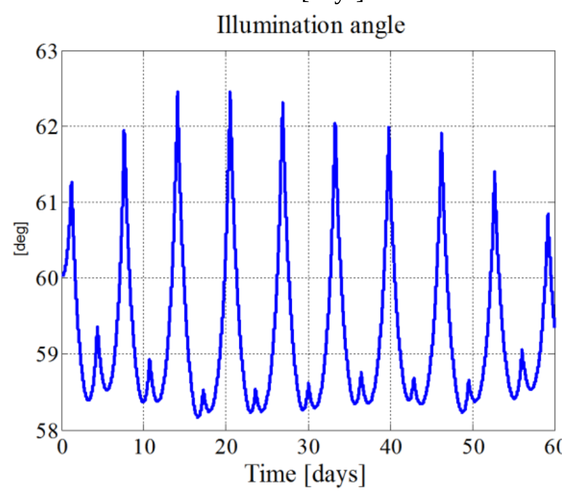

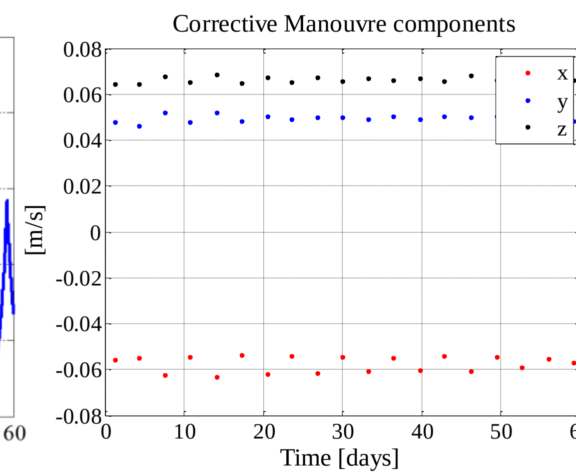

Station Keeping at 10 km Station for AIM

Synthetic results displayed: single case

Total control budget is: 1.9154 m/s

Mean Time between actuations: 4547.3684 min
Min Time between actuations: 4392.0903 min
Max Time between actuations: 4858.802 min

MC simulation

- 20 m along track (1σ)
- 10 m cross (1σ)
- 2 mm/s along track (1σ)
- 1 mm/s along track (1σ)
- 50 m per component position dispersion (1σ)
- 1 cm/s per component velocity dispersion (1σ)
- 2% (3σ) error in magnitude
- 1.5 deg (3σ) error in direction

MC statistics (30 days)

Total control budget is: 0.93109 m/s (dispersion 1-σ: 0.048834 m/s)

Mean Time between actuations: 3.1824 days (dispersion 1-σ: 0.03609 days)
Min mean Time between actuations: 3.0032 days (dispersion 1-σ: 0.087042 days)
Max mean Time between actuations: 3.3528 days (dispersion 1-σ: 0.068887 days)

Min mean dv actuations: 0.042674 m/s (dispersion 1-σ: 0.0023174 m/s)
Max mean dv actuations: 0.067255 m/s (dispersion 1-σ: 0.0010453 m/s)

Minimum and maximum manoeuvre vs. minimum actuation time

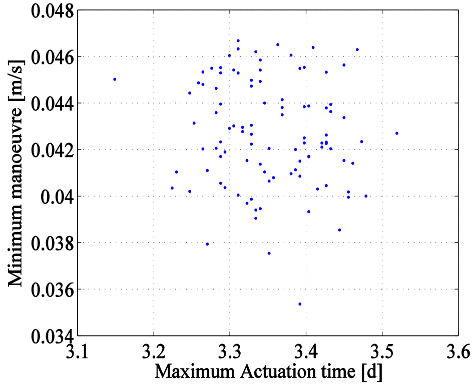

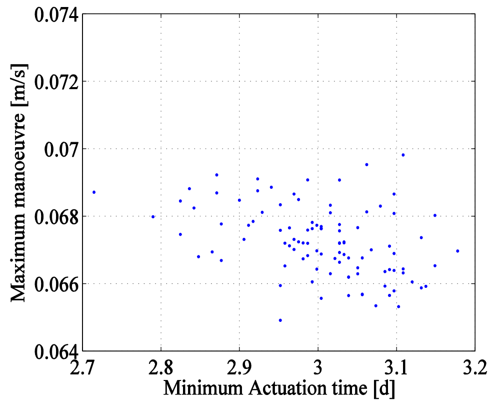

Deflection Module

❑ Laser Ablation

- 3D Interaction laser-matter (Thiry et al 2015)
- Thrust aligned to local surface normal
- Affected by rotational velocity
- No contamination included
- 2 laser pointing strategies
  - Pointing to obtain desired thrust direction
  - Fixed laser pointing

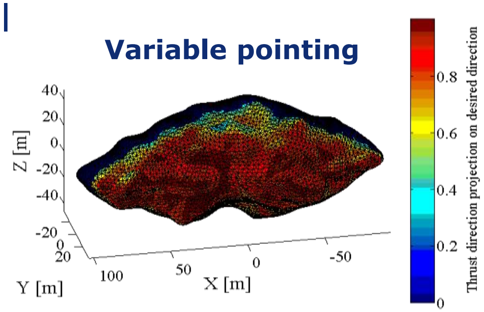

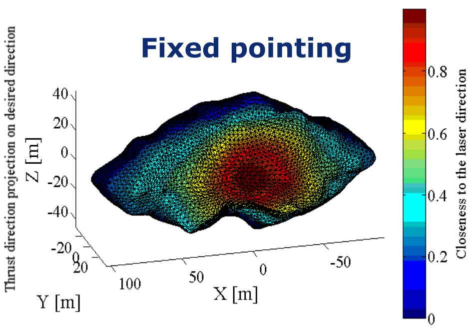

❑ Ion Beam shepherd

- Ion plume Gaussian expansion (Goebel et al 2008)
- Ion plume constant axial velocity
- 2 thrusters required
- No contamination included

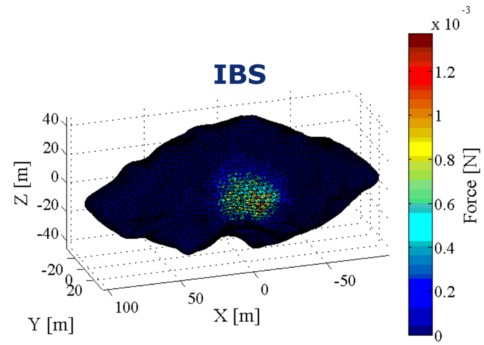

❑ Gravity Tractor

- Avoid asteroid impingment by expansion plume

❑ Orbital and rotational dynamics computational intensive:

- Mean directions of thrust and efficiency based on the actual geometry of the asteroid over a control period of 7 days
- Variational approach implemented (Gauss equations)
- No actual spacecraft control integrated

Deflecting a 100 m Asteroid

- (433) Eros scaled down to 100 m
- mass $9.263 \cdot 10^8$ kg
- 20 years operations
- 20 kW maximum power for laser beam (μ=50%) or thrusters (μ= 60%)
- Systems placed at 200 m along track

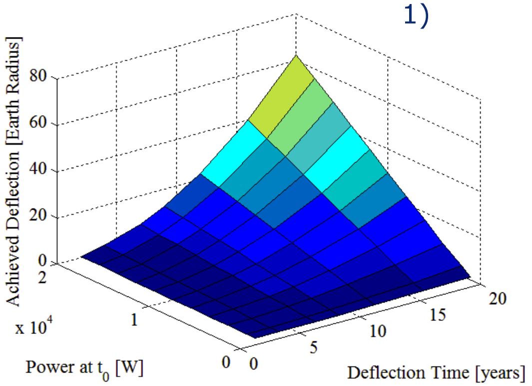

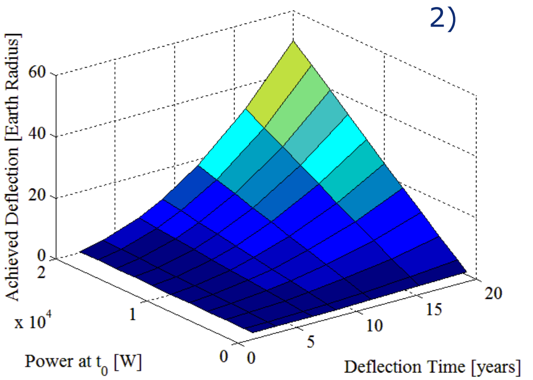

Laser ablation deflection: 1) controlling laser pointing, 2) maintaining laser pointing fixed.

Results

- GT Maximum deflection
  - spacecraft mass circa 16500 kg
- LA with variable pointing 20% more efficient than the fixed pointing
  - operationally more complex
- IBS appears less efficient but
  - more lightweight and less affected by contamination

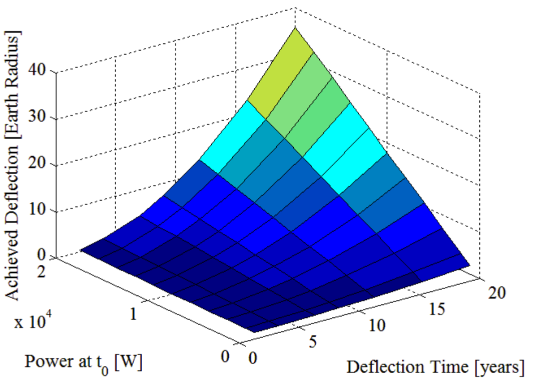

Ion Beam Shepherd deflection

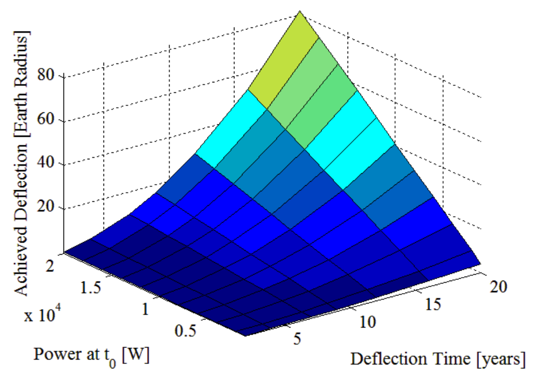

Gravity Tractor deflection.

Debris Analysis around a 100 m Asteroid

- ❑ Possible impact on a 100 m asteroid
- ❑ Time to clear the proximity of the asteroid

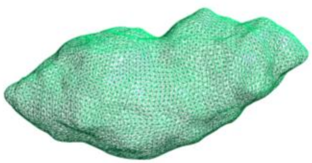

Hill radius: circa 15 km
Asteroid 2013XK22: Shape Geographos

$$[a, e, i, \Omega_a, \omega_a] = [1.045\mathrm{AU}, 0.2034, 0.1221\mathrm{rad}, 3.187\mathrm{rad}, 4.6374\mathrm{rad}]$$

- 30,000 uniformly distributed samples on the surface E≤0
- different value of area to mass ratios (A2M)
- fractions k_ω of the asteroid's nominal angular velocity

❑ The **initial conditions** play important role in the number of surviving particles; if all the SRP is the same, particles with lower initial tangential velocity will have more probability to survive for longer period

❑ The **SRP** will affect the survivability – A2M = 0.001 kg/m^2 produces more surviving samples because particles are more affected by the asteroid's gravity and less by the SRP

❑ At the beginning the particles with higher energy (close to 0) will experience **SRP and third body** effects leading to escape/impact

Survival particles from impact

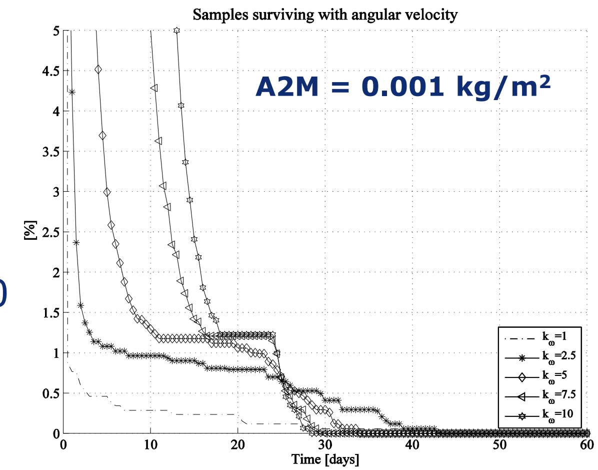

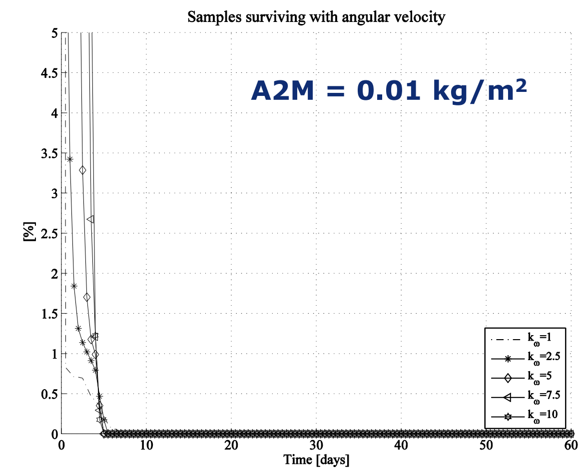

Conclusions & Future Works

- Main features and architecture of HADES
  - Dynamics in 3 different frames
  - Several control techniques available
  - Different measurement models
  - Use of asteroid actual shapes
  - GNC
  - Deflection analysis

- Possibility of performing broad range of simulations
  - Assessment different control laws
  - Assessment impact of environment knowledge
  - MC simulations
  - Debris analysis
  - LA, IBS and GT deflections

- Improvements
  - Integration of deflection systems
    - Propagation Module
    - Control Module
    - Navigation Module
      - Estimation of the deflective action
  - Effect of contamination

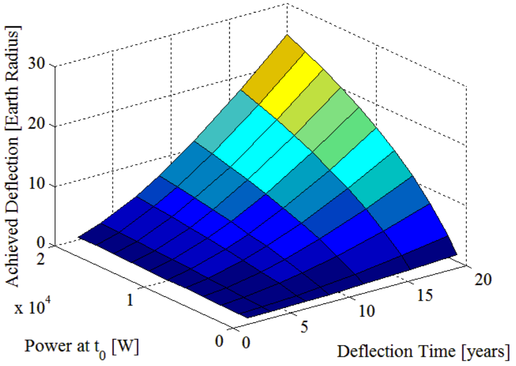

LA laser pointing control with contamination

Thank you

EU FP7 funded Stardust project
Marie Curie Initial Training Network
Grant Agreement 317185
www.stardust2013.eu
twitter.com/stardust2013eu

References

1. T. Kubota, T. Hashimotoa, S. Sawai, J. Kawaguchib, K. Ninomiyaa, M. Uoc, K. Babac, "*An autonomous navigation and guidance system for MUSES-C asteroid landing*", Acta Astronautica 52 (2003) 125 – 131.
2. S. Li, P. Cui and H. Cui, "Autonomous navigation and guidance for landing on asteroids", Aerospace science and technology, 10(3): 239-247, 2006
3. H.J. Melosh, I.V. Nemchinov and Y.I. Zetzer, "Non-nuclear strategies for deflecting comets and asteroids", In: Gehrels, T. (Ed.), Hazard due to comets and asteroids. University of Arizona Press, pp. 1111–1132, 1994.
4. C. Colombo, J.P. Sanchez Cuartielles, M. Vasile et al, "A comparative assessment of different deviation strategies for dangerous NEO", International Astronautical Congress. Valencia, Spain, October, 2006.
5. A. Galvez et al, "Asteroid Impact Mission (AIM) & Deflection Assessment: An Opportunity to Understand Impact Dynamics and Modelling", European Planetary Science Congress 2012, in Madrid, Spain,23-28 September, 2012.
6. Montenbruck, O. and Gill, E., Satellite Orbits: Models, Methods and Applications, Springer-Verlag, Heidelberg, 2005.
7. T. Winkler, B. Kaplinger and B. Wie, "Optical Navigation and Fuel-Efficient Orbit Control Around an Irregular-Shaped Asteroid", AIAA Guidance, Navigation, and Control (GNC) Conference, Boston, USA, 08/2013.
8. W. Boyce, "Comment on a formula for the gravitational harmonic coefficients of a triaxial ellipsoid", Celestial Mechanics and Dynamical Astronomy, , Volume 67, Issue 2, pp 107-110, February 1997
9. M. Vasile and C.A. Maddock. "Design of a Formation of Solar Pumped Lasers for Asteroid Deflection", Advances in Space Research, 2012, 50(7): 891-905, 2012
10. S. B. Broshart and D. J. Scheeres. "Boundness of Spacecraft Hovering under Dead-Band Control in Time-Invariant systems", Journal of Guidance, Control and Dynamics Vol. 30, March-April 2007.
11. Y. Liu et al., 2003. "Stability Analysis of Impulsive control systems", Mathematical and Computational Modelling 37 (2003) 1357-1370), 2003.
12. Simons, D., Optimal state estimation, Kalman, and Non-linear Approaches, Published by John Wiley & Sons, Inc., Hoboken, New Jersey, 2006.
13. W. Li, and Y. Jia, "H-infinity filtering for a class of nonlinear discrete-time systems based on unscented transform", Signal Processing 90(2010)3301–3307, 2010.
14. S.M Oh and E.N. Johnson, "Relative Motion Estimation for Vision-based Formation Flight using Unscented Kalman Filter", AIAA Guidance, Navigation and Control Conference and Exhibit, Hilton Head, South Carolina, 2007.
15. K. Dionne, "Improving Autonomous Optical Navigation for Small Body Exploration Using Range Measurements", AIAA 2009-6106. AIAA Guidance, Navigation, and Control Conference, 10 - 13 August 2009, Chicago, Illinois.
16. N. Thiry and M. Vasile, "Deflection of uncooperative targets using laser ablation", in SPIE Optical Engineering + Applications. International Society for Optics and Photonics, 2015.
17. Goebel D. M. and Katz Ira. Fundamentals of Electric Propulsion: Ion and Hall Thrusters, JPL SPACE SCIENCE AND TECHNOLOGY SERIES. Chapter 1 and 8., March 2008.
18. C. Colombo, M. Vasile and G. Radice, "Semi-Analytical Solution for the Optimal Low-Thrust Deflection of Near-Earth Objects", Journal of Guidance Control and Dynamics 32(32):796-809, May 2009.

Control Module

$$\delta\dot{x} = \begin{bmatrix} 0_{3x3} & I_{3x3} \\ -\frac{\mu_a}{\delta r_0^3}[I - 3\hat{r}_0\hat{r}_0] & 0_{3x3} \end{bmatrix}\delta x + \begin{bmatrix} 0_{3x3} \\ I_{3x3} \end{bmatrix} u = \begin{bmatrix} 0_{3x3} & I_{3x3} \\ \beta & 0_{3x3} \end{bmatrix}\delta x + \begin{bmatrix} 0_{3x3} \\ I_{3x3} \end{bmatrix} u \qquad \delta x_{k+1} = \begin{bmatrix} I + \beta\frac{\Delta t^2}{2} & \Delta t I_{3x3} \\ \beta\Delta t & I_{3x3} \end{bmatrix}\delta x_k + \begin{bmatrix} \Delta t I_{3x3} \\ I_{3x3} \end{bmatrix} u_k = A_k \delta x_k + B_k u_k$$

- Discrete LQR with integrative contribution

$$J(\mathbf{u}) = \sum_{k=1}^{\infty} x_k^T Q x_k + \mathbf{u}_k^T \mathbf{R} \mathbf{u}_k \qquad K = (B_k^T S B_k + R)^{-1} \mathbf{B}_k^T \mathbf{S} \mathbf{A}_k \qquad A_k^T S^T A_k - S - A_k^T S A_k \left(B_k^T S B_k\right)^{-1} B_k^T S A_k + Q = 0$$

- Discrete control designed using stability criteria (Y. Liu et al, 2003)

$$\begin{aligned} \dot{\mathbf{x}} &= f(t, x) & t &\neq t_k \\ \mathbf{z} &= h(\mathbf{x}) & t &\neq t_k \\ \Delta\mathbf{x} &= \mathbf{u_k}(\mathbf{x}) & t &= t_k \\ \mathbf{x}(\mathrm{t}_0) &= \mathbf{x}_0 & t &= t_0 \end{aligned}$$

– *f* and *h* are null for $x = 0$

$$V(t, x) \leq a(\|x\|)$$

$$V(t, x) = \frac{1}{2}(x^2 + y^2 + z^2 + T^2 v_x^2 + T^2 v_y^2 + T^2 v_z^2)$$

1- There has to exist a constant l_k

$$D^+V(t, x) \leq \frac{l_k}{\Delta t_k} c_k(V(t, x)) \qquad \gamma = \frac{l_k}{\Delta t_k}$$

D^+ is the right-hand generalized derivative

Δt_k control time

$c_k(\ldots)$ suitable scalar function

$$u_k(\delta\mathbf{x}) = [0{,}0{,}0, -ax - av_x, -ay - bv_y, -az - bv_z]^T$$

$$D^+V(t, x) = xv_x + yv_y + zv_z + \beta_1 T^2 x v_x + \beta_2 T^2 y v_y + \beta_3 T^2 z v_z \leq \gamma\frac{1}{2}(x^2 + y^2 + z^2 + T^2 v_x^2 + T^2 v_y^2 + T^2 v_z^2)$$

2- There has to exist a constant

$$V(t_k^+, x + u_k) \leq V(t_k, x) + v_k d_k(V(t, x))$$

$$l_k + v_k \leq 0$$

for suitable neighbourhood of $s(\varrho) / \|x\| \leq \varrho$

$$c_k(s) \leq d_k(s) \quad \text{if} \quad v_k < 0$$

and $d_k(s) \leq c_k(s)$ if $l_k < 0$

$$s + v_k d_k(s) \leq 0 \qquad d_k(s) = c_k(s) = s$$

$$V(t_k^+, x + u_k) = \frac{1}{2}\left(x^2 + y^2 + z^2 + T^2(v_x + ax + bv_x)^2 + T^2\left(v_y + ay + bv_y\right)^2 + T^2(v_z + az + bv_z)^2\right) \leq \gamma\frac{1}{2}\gamma\frac{1}{2}(x^2 + y^2 + z^2 + T^2 v_x^2 + T^2 v_y^2 + T^2 v_z^2)$$

$$x^T A x \geq 0$$

Infos

- ❑ HADES runs completely in **matlab**
- ❑ **Routines** both in Matlab® and **mex-fied in C for speed purpose**
  - ✓ dynamics equations (mainly for gravity field purposes)
  - ✓ visibility functions (shapes, shadows)
- ❑ Integration of ODE
  1. matlab ode **Runge-Kutta 45** (for events to be located)
  2. integrator **ODEMEXv12** package
     - ✓ 10-50 times faster
     - X No events handling
     - X asteroid shape dynamcs to be included
- ❑ Hints
  - Coupled Control-Navigation intensive
    - ➢ performance methods for long simulations
    - ➢ simulations to draw necessary statistics

    and move to performance model
  - Continuous, discrete LQR and control box tends to be more precise and robust

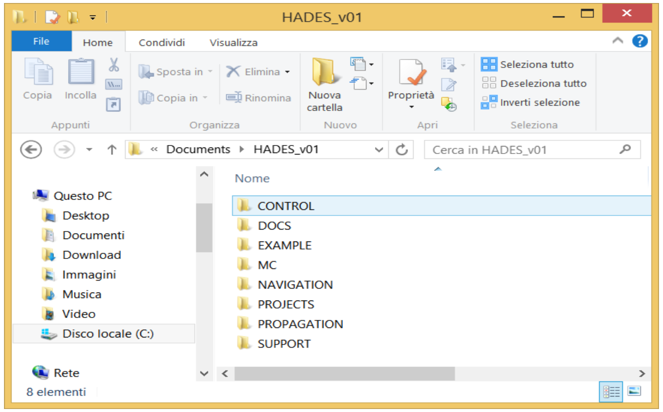

Gravity Based on Polyhedral Model

Potential gradient defined using polyhedron described by triangular facets

$$\nabla U = -G\rho \sum_{e\in edges} L_e \tilde{E}_e \cdot \vec{r}_e + G\rho \sum_{f\in facets} \omega_f \tilde{F}_f \cdot \vec{r}_f$$

$$\tilde{E}_e = \vec{n}_A \vec{n}^A_{21} + \vec{n}_B \vec{n}^B_{12}$$

$$\tilde{F}_f = \vec{n}_f \vec{n}_f$$

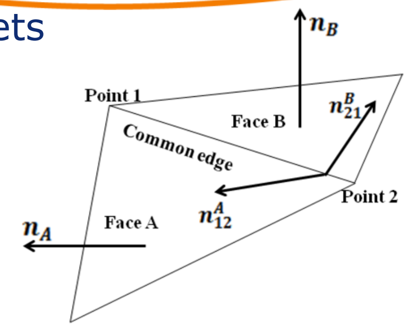

Geometrical characterisation of the surface (normals, edges etc)

$$L_e = \ln \frac{r_i + r_j + e_{ij}}{r_i + r_j - e_{ij}}$$

$$\omega_f = 2 \arctan \frac{\vec{r}_i \cdot \vec{r}_j \times \vec{r}_k}{r_i r_j r_k + r_i(\vec{r}_j \cdot \vec{r}_k) + r_j(\vec{r}_k \cdot \vec{r}_i) + r_k(\vec{r}_i \cdot \vec{r}_j)}$$

$\mathbf{r}_f$ spacecraft distance from facet's centre

$\mathbf{r}_e$ spacecraft distance from edge centre

Asteroid (433) Eros - acceleration on the surface: comparison with paper Winkler

Winkler

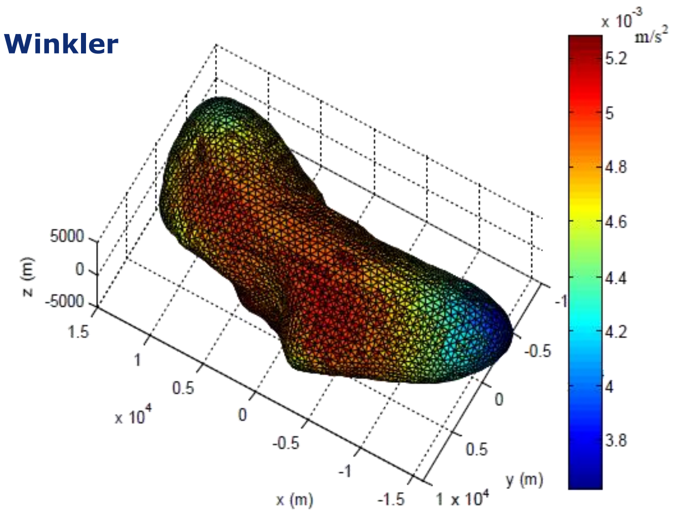

Implemented model

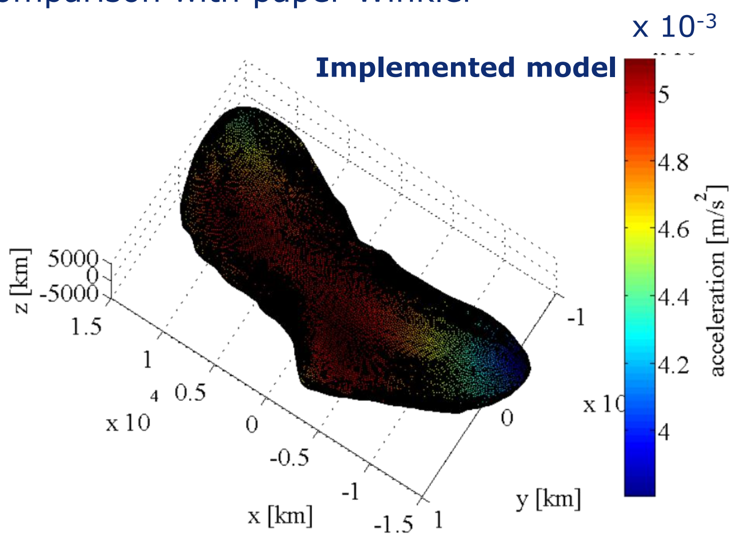

Solution overlapping – difference due to number of facets and density (assumed 2500 kg/m³)

Spherical Harmonics and Reflection

Ellipsoid of arbitrary size: harmonics coefficients (Boyce 1997)

$$C_{2n,2m} = \frac{3}{R^{2n}} \frac{n!(2n-2m)!}{2^{2m}(2n+3)(2n+1)!}(2-\delta_{0m}) \sum_{i=0}^{\mathrm{int}(\frac{n-m}{2})} \frac{(a^2-b^2)^{m+2i}[c^2-1/2(a^2+b^2)]^{n-m-2i}}{16^i(n-m-2i)!(m+i)!i!}$$

Gravity attraction error on the circumscribing sphere at 3 km mesh 14400 facets

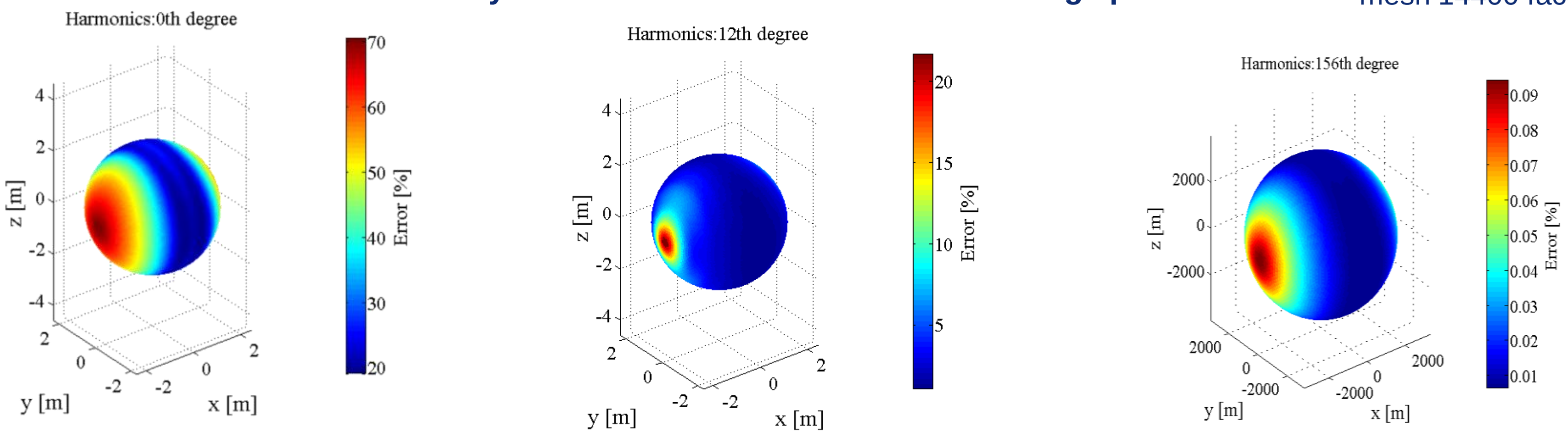

Reflection: unable to maintain 5 degrees illumination angle